Environ. Sci. Technol. **2006**, *40,* 4109−4118

Size-Resolved Emissions of Organic Tracers from Light- and Heavy-Duty Vehicles Measured in a California Roadway Tunnel

HARISH C. PHULERIA, MICHAEL D. GELLER, PHILIP M. FINE, AND CONSTANTINOS SIOUTAS*

Department of Civil and Environmental Engineering, University of Southern California, Los Angeles, California 90089

Individual organic compounds found in particulate emissions from vehicles have proven useful in source apportionment of ambient particulate matter. Species of interest include the hopanes, originating in lube oil, and selected PAHs generated via combustion. Most efforts to date have focused on emissions and apportionment PM_{10} or $PM_{2.5}$. However, examining how these compounds are segregated by particle size in both emissions and ambient samples will help efforts to apportion size-resolved PM, especially ultrafine particles which have been shown to be more potent toxicologically. To this end, high volume size-resolved (coarse, accumulation, and ultrafine) PM samples were collected inside the Caldecott tunnel in Orinda, California to determine the relative emission factors for these compounds in different size ranges. Sampling occurred in two bores, one off-limits to heavy-duty diesel vehicles, which allows determination of the different emissions profiles for diesel and gasoline vehicles. Although tunnel measurements do not measure emissions over a full engine duty cycle, they do provide an average emissions profile over thousands of vehicles that can be considered characteristic of "freeway" emissions. Results include size-fractionated emission rates for hopanes, PAHs, elemental carbon, and other potential organic markers apportioned to diesel and gasoline vehicles. The results are compared to previously conducted $PM_{2.5}$ emissions testing using dynamometer facilities and other tunnel environments.

Introduction

Motivated by the growing concern that human exposure to ultrafine particles poses a significant health hazard, characterization of particles emitted from gasoline and diesel engines has been the focus of many studies (*1*−*3*). Vehicular particulate emissions are of specific interest because of their potentially toxic components, such as polycyclic aromatic compounds (PAHs) and trace metallic elements. A number of health studies have demonstrated the adverse health effects of diesel exhaust particles (*4*−*6*).

The recent focus on the smaller vehicle-derived ultrafine particles has been due to their higher number and surface area relative to larger particles, their ability to penetrate cell membranes, and to their increased toxicity on a per mass basis (*7*, *8*). Li et al. (*7*) have shown that ultrafine particles (defined in this case as those having diameters less than about 180 nm) induce a higher degree of oxidative stress and cause more cell damage than an equivalent mass of fine particles (aerodynamic diameter < 2.5 μm). Animal exposure studies have further corroborated increased adverse health outcomes from ultrafine airborne particles (*9*−*13*).

Since ultrafine particle number and mass do not necessarily correlate with mass concentrations of larger particles (PM_{10} or $PM_{2.5}$) (*14*−*16*), these more common measurements cannot be used for information on ultrafine particle concentrations. Given the results of the recent health studies that may drive future regulatory strategies, it is essential that the sources of and the human exposure to vehicular ultrafine particle emissions are well understood (*17*, *18*).

Several different approaches have been applied for examining vehicular emissions, including roadside measurements (*19*), on-road chase experiments (*20*, *21*), laboratory dynamometer studies (*22*−*26*), and measurements inside roadway tunnels (*2*, *27*−*32*). Dynamometer and chase experiments are useful due to the ability to carefully control testing conditions. Emissions control technologies can be evaluated, and emissions differences over different driving conditions and cycles, including cold-start (*33*), can be examined. However, the high cost and complexity of such tests limit the number of vehicles which can be assessed, and thus may not provide a good representation of the vehicle fleet composition on the road. Moreover, changing the dilution conditions in dynamometer testing is known to affect the measurements, especially for ultrafine particles (*34*). Such studies may not account for particle aging effects, the mixing of emissions from different vehicles (*6*), and nontailpipe emissions from tire wear, brake wear, and re-suspended road dust (*27*).

An alternative to single-vehicle emission measurements is roadway tunnel studies measuring the emissions from a large population of the on-road vehicle fleet mix under real-world driving conditions. Roadside measurements will sample under actual ambient conditions, but are subject to wind and other environmental processes, which might vary the emissions and background conditions (*22*). Although the dilution, temperature, humidity, and sunlight conditions inside a tunnel may differ from conditions outside tunnels, they more closely approximate real-world conditions than dynamometer tests. Air is directly sampled from inside the tunnel bore, very high concentrations are encountered, and thus, practically all measurements can be attributed to vehicles (*35*). In tunnels with multiple bores that have traffic restrictions based on vehicle size, such as the Caldecott tunnel in California (*2*, *31*, *32*), apportionment of emissions to vehicle or fuel type can be achieved (*22*). A limitation of tunnel measurements is that they measure emissions over the very specific driving conditions of the particular tunnel, missing cold-start emissions and some transient effects. However, a highway tunnel can provide detailed emissions characterization under typical highway driving conditions, resulting in a real-world average highway source signature. The derived vehicular PM emission factors are important in assessing effects on human exposure and health (*36*, *37*).

Several studies have measured individual organic compounds in atmospheric particulate matter (PM) samples. Using gas chromatographic/mass spectrometric methods, hundreds of particle-phase individual compounds have been identified and quantified in ambient air (*15*, *38*−*42*). Usually, only between 10 and 20% of the total particulate organic compound mass can be quantified as individual organic

* Corresponding author e-mail: sioutas@usc.edu.

10.1021/es052186d CCC: $33.50
Published on Web 05/26/2006

species, but many of these compounds have been used to trace primary particle emissions via source apportionment techniques (*39*, *40*, *42*). Accurate and up-to-date source profiles are essential for the successful application of these methods. Specific organic tracers of primary vehicular particle sources include hopanes and steranes, found in the lubricating oils used by both gasoline- and diesel-powered motor vehicles (*23*, *39*, *43*). High molecular weight PAHs have also been used as tracers for motor vehicle exhaust, although there are additional combustion sources of PAHs including wood combustion (*23*, *43*, *44*). Miguel et al. (*32*) reported that gasoline-powered vehicles are a significant source of the higher molecular weight PAHs such as benzo(ghi)-perylene, while diesel vehicles predominantly emit the lighter PAHs, such as fluoranthene and pyrene. Diesel engines are known to have significantly higher elemental carbon (EC) emissions than gasoline-powered vehicles (*24*, *39*, *45*). It may be possible, therefore, that information on emissions of high and low molecular weight PAHs, hopanes, steranes, and EC from motor vehicles can be used to distinguish between diesel and gasoline vehicle contributions to ambient samples in chemical mass balance source apportionment calculations (*46*, *47*). Another potential vehicular marker is the unresolved complex mixture (UCM) of hydrocarbons, appearing as an unresolved hump underlying identifiable compound peaks in typical GC/MS traces (*48*, *49*). The ion spectra of the UCM look very similar to that of typical motor oil (*24*). To the extent that vehicle derived UCM can be accurately quantified in emission and ambient samples, it may serve as an additional indicator of vehicular particulate emissions.

A few previous studies have measured size-fractionated PAH, oxy-PAH, and organonitrates over 5−24 h periods (*50*−*53*). However, most ambient and emissions samples intended for organic speciation are not size-resolved, due to limitations in collecting sufficient particle mass for trace species analysis. A high-volume slit impactor developed by Misra et al. (*54*) allows for separation of particles based on aerodynamic diameter with a cut-off point of 0.18 μm and a flow rate of 450 Lpm. The impactor, with a high-volume after-filter, has been successfully deployed to collect separate ultrafine (<0.18 μm) and accumulation mode (0.18−2.5 μm) ambient samples in Los Angeles (*15*).

The current study was conducted within two bores of the Caldecott tunnel in Orinda, CA during August and September of 2004. The high-volume slit impactor was deployed to collect size-resolved PM (ultrafine and accumulation mode) for speciated organic analysis of vehicular emissions by GC/MS. The emissions characterization for bulk species, such as mass, elemental carbon (EC), organic carbon (OC), and trace elements, from this campaign has been reported previously (*2*). This work provides additional detailed information on organic tracers of real-world vehicular sources found in the two different PM size ranges. The first reported size-segregated emission factors for organic tracers, other than PAH, are calculated for both gasoline-powered light-duty vehicles (LDV) and diesel-powered heavy-duty vehicles (HDV). Emission factor results for $PM_{2.5}$ are compared to those of previous tunnel and dynamometer studies. Combined with other source profiles, including that of vehicular cold-start emissions, the results can be used in future chemical mass balance calculations to assess the relative contribution of PM sources to ambient samples.

Experimental Procedures

Tunnel Sampling. A detailed description of the tunnel environment, traffic characteristics, and sampling procedure is described by Geller et al. (*2*). Briefly, the 1.1-km long Caldecott Tunnel in Orinda, CA includes three two-lane bores with a 4.2% incline from west to east (*2*, *27*, *30*, *55*). Bores 1 and 3 allow both light-duty vehicles (LDV) and heavy-duty vehicles (HDV), while bore 2 is restricted to LDV traffic only. Traffic flows from west-to-east in Bore 1, east-to-west in Bore 3, and the direction of traffic switches from westward in the morning to eastward in the afternoon and evening in Bore 2. Field sampling was conducted in the afternoon in Bores 1 and 2 for 4 days each from approximately 12 p.m. to 6 p.m., when all traffic in the two bores traveled eastward, during August and September of 2004.

Traffic Characterization. The traffic volume and vehicle characteristics in the tunnel during the sampling campaign are also described by Geller et al. (*2*). (see Table S1, Supporting Information). Although Bore 2 is legally restricted to light-duty traffic, some medium-duty diesels and an occasional heavy-duty three-axle vehicle passed through. The method for attributing 2-axle/6-tire vehicles to gasoline and diesel fuel is given in Geller et al. (*2*). As a percentage of the total vehicles counts, diesel vehicles are an order of magnitude less prevalent in Bore 2 than in Bore 1. During the sampling campaign, heavy-duty vehicles comprised an average of 3.8% of the total vehicles in bore 1 and less than 0.4% of vehicles in bore 2.

Pollutant Measurement and Sample Collection. Both gaseous and particulate pollutant concentrations in the tunnel bores were measured with various continuous and time-integrated instruments, approximately 50 m from the tunnel exit and 50 m from the tunnel entrance. Since the entrance location was also inside the tunnel, it is not a pure ambient background sample, considering that it includes roadway emissions from the first 50 m of the tunnel. Emission factors are calculated based on the difference in concentrations between exit and entrance samples over a known, fixed distance of roadway between sampling locations.

PM collection was accomplished with a custom built, high-volume (450 Lpm) sampler designed to separate and collect coarse (Dp > 2.5 μm), accumulation (0.18 < Dp < 2.5 μm), and ultrafine mode (Dp < 0.18 μm) aerosols (*54*). It allows collection of particles with aerodynamic diameters greater than about 180 nm onto quartz-fiber impaction strips. A preceding impaction stage with a 2.5 μm aerodynamic diameter cut-off point removes coarse particles. Downstream of the ultrafine impactor, a commercially available 8 × 10 in. high-volume filter holder contains a Quartz-fiber filter (Pallflex Tissuquartz 2500QAT-UP-8 × 10, Pall Corp.) to collect the ultrafine PM fraction. Field blanks for quartz filters contained negligible levels of the compounds quantified in this study. Quartz filters and substrates were prebaked at 550 °C for 12 h and stored in baked aluminum foil prior to deployment (*2*, *15*).

Organic Speciation Analysis. Methods for the quantification of individual organic compounds in ambient particulate matter were based on the procedures initially developed by Mazurek et al. (*56*) and advanced further by others (*15*, *24*, *25*, *57*). The quartz filter samples from the high-volume sampler were cut into smaller portions and combined in an annealed glass jar with a Teflon-lined lid. Samples were then spiked with known amounts of isotope-labeled internal standard compounds, including three deuterated PAHs, two deuterated alkanoic acids, deuterated cholestane, deuterated cholesterol, and C^{13}-labeled levoglucosan. Solvent extraction of all samples was performed with three successive 10-minute mild sonications in 50 mL of a 9:1 mixture of HPLC-grade dichloromethane and methanol. The 50 mL extracts from each sonication step were then combined and reduced in volume to approximately 10 mL by rotary evaporation at 35 °C under a slight vacuum. The remaining volume was filtered through a baked quartz-fiber filter, and then reduced to approximately 1 mL under pure nitrogen evaporation before the samples were split into two separate fractions. One fraction was derivatized for organic acid analysis, the results of which are not presented here. The other fraction was

TABLE 1. Pearson Correlation Coefficient between Mass Concentrations of Various Measured Species in Ultrafine and Accumulation Modes

	EC	PAH = 226 + 228 MW[a]	PAH = 252 MW[b]	BgP	Cor	PAH ≥ 276 MW[c]	sum Hop-Ster[d]	UCM
Ultrafine Mode								
EC	1.00							
PAH = 226+228 MW	0.98	1.00						
PAH = 252 MW	0.95	0.98	1.00					
BgP	0.84	0.91	0.96	1.00				
Cor	0.56	0.64	0.73	0.88	1.00			
PAH >= 276 MW	0.79	0.86	0.92	0.99	0.93	1.00		
Sum Hop-Ster	0.96	0.97	0.95	0.91	0.74	0.89	1.00	
UCM	0.96	0.99	0.99	0.94	0.70	0.90	0.96	1.00
Accumulation Mode								
EC	1.00							
PAH = 226 + 228 MW	0.78	1.00						
PAH = 252 MW	0.83	0.97	1.00					
BgP	0.65	0.95	0.91	1.00				
Cor	0.36	0.72	0.64	0.87	1.00			
PAH ≥ 276 MW	0.59	0.92	0.88	1.00	0.90	1.00		
Sum Hop-Ster	0.76	0.99	0.96	0.94	0.73	0.91	1.00	
UCM	0.80	0.99	0.96	0.93	0.70	0.90	0.99	1.00

[a] Sum of benzo(ghi)fluoranthene, benz[*a*]anthracene, and chrysene/triphenylene. [b] Sum of benzo[*k*]fluoranthene, benzo[*b*]fluoranthene, benzo[*j*]fluoranthene, benzo[*e*]pyrene, benzo[*a*]pyrene, and perylene. [c] Sum of indeno(cd)pyrene, benzo(ghi)perylene, indeno(cd)fluoranthene, and coronene. [d] Sum of hopanes and steranes.

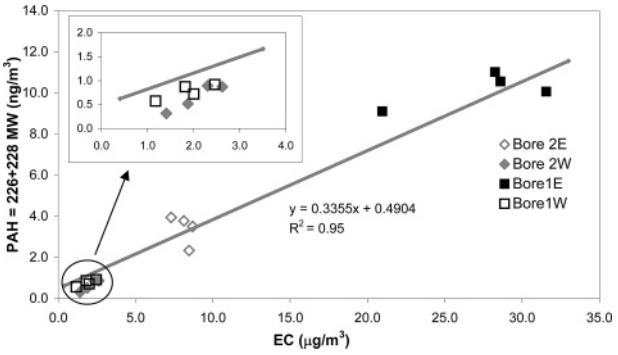

FIGURE 1. Correlation plot between mass concentrations of EC and Sum PAHs with MW 226 and 228 in ultrafine mode.

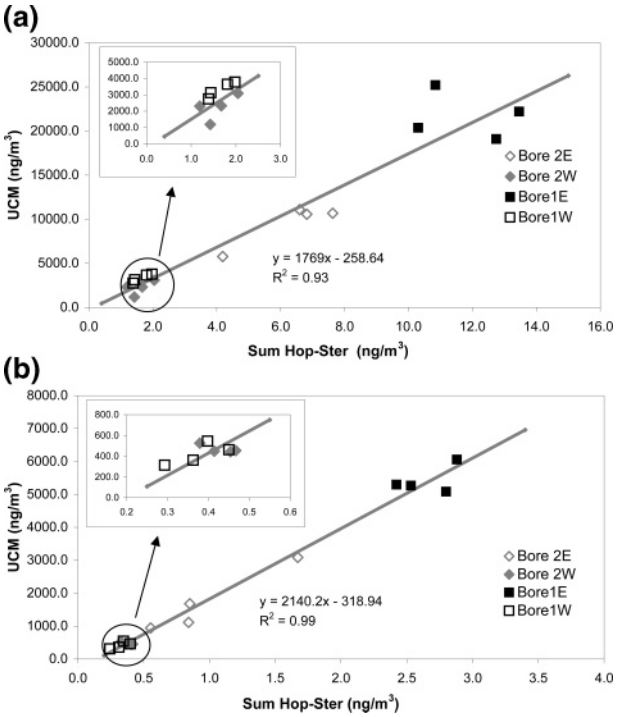

FIGURE 2. Correlation plot between mass concentrations of Sum Hop-Ster and UCM in (a) ultrafine mode and (b) accumulation mode.

further reduced to a specified volume ranging from 50 to 200 μL by evaporation under pure nitrogen. The final target volume was determined based on the amount of organic carbon mass in each sample (*15*, *58*).

The underivatized samples were analyzed by auto-injection into a GC/MSD system (GC model 5890, MSD model 5973, Agilent). A 30 m × 0.25 mm DB-5MS capillary column (Agilent) was used with a 1 μL splitless injection. Along with the samples, a set of authentic quantification standard solutions were also injected and used to determine response factors for the compounds of interest. The standard mixtures included known amounts of the same isotope-labeled compounds used to spike the samples. Each standard compound is assigned a response factor relative to one of the internal standards with a similar retention time and structure. Between one and three of the most prevalent ions in the spectrum for each compound were selected for peak integration. While some compounds are quantified based on the response of a matching compound in the standard mixtures, others for which matching standards were not available are quantified using the response factors of compounds with similar structures and retention times. UCM quantification was based on the total ion current (TIC) response of standard alkanes with similar retention times. Analytical errors for these methods have been reported to be no more than 25% (*15*, *42*, *57*).

Emission Factors. Fuel-based emission factors relating total carbon emissions in the tunnel (primarily in the form of CO_2) to the carbon content of fuel are computed as described in detail by Kirchstetter et al. (*30*) and were applied in the previous paper from this sampling campaign (*2*). Briefly, pollutant concentrations are expressed as mass emitted per unit mass of fuel burned by the following equation:

$$E_p = 10^3\left(\frac{\Delta[P]}{\Delta[CO_2] + \Delta[CO]}\right)w_c$$

where E_p is the emission factor (g emitted per kg fuel burned) for pollutant P, $\Delta[P]$ is the increase in the concentration of pollutant P ($\mu g/m^3$) above the tunnel entrance location, $\Delta[CO_2]$ and $\Delta[CO]$ are the increases in the concentrations

TABLE 2. Emission Factors (in μg/kg Fuel Burned) Attributable to LDVs and HDVs in Ultrafine and Accumulation Mode[a]

	LDV				HDV			
	ultrafine		accumulation		ultrafine		accumulation	
sample ID	mean	SD	mean	SD	mean	SD	mean	SD
fluoranthene	2.39	0.43	0.37	0.13	114.90	33.16	21.93	4.50
acephenanthrylene	0.43	0.05	0.05	0.01	25.91	6.93	4.18	1.23
pyrene	3.63	0.68	0.55	0.20	206.47	60.03	36.23	7.10
methyl substituted MW 202 PAH	3.75	2.34	0.44	0.40	233.54	61.53	29.52	5.10
benzo(ghi)fluoranthene	3.55	0.78	0.44	0.14	89.99	11.04	11.32	0.55
benz[*a*]anthracene	4.11	0.76	0.43	0.13	65.69	13.80	7.30	0.46
chrysene/triphenylene	4.43	1.03	0.50	0.19	51.52	15.64	7.33	0.52
methyl substituted MW 228 PAH	3.09	0.95	0.25	0.22	40.19	3.00	4.94	0.61
benzo[*k*]fluoranthene	3.75	1.40	0.36	0.09	43.41	9.37	4.47	1.95
benzo[*b*]fluoranthene	4.75	1.35	0.46	0.15	59.34	11.17	7.11	2.34
benzo[*j*]fluoranthene	0.99	0.34	0.06	0.00	11.29	3.27	1.17	0.44
benzo[*e*]pyrene	4.42	1.40	0.41	0.11	60.80	15.28	6.36	2.29
benzo[*a*]pyrene	5.08	1.56	0.34	0.04	46.76	18.55	4.04	1.13
perylene	0.74	0.24	0.06	0.04	9.92	1.37	1.76	1.31
indeno(cd)pyrene	3.79	1.36	0.28	0.09	8.52	4.20	1.49	0.87
benzo(ghi)perylene	9.63	2.76	0.68	0.22	47.90	23.47	4.96	1.40
indeno(cd)fluoranthene	1.26	0.44	0.08	0.03	6.53	3.67	0.59	0.15
dibenz[a,h]anthracene	0.29	0.07	0.04	0.02	0.92	0.31	0.48	0.64
coronene	5.32	1.00	0.24	0.09	5.74		0.68	0.38
22,29,30-trisnorhopane	1.56	0.36	0.23	0.17	13.27	2.46	4.53	0.13
22,29,30-trisnorneohopane	1.38	0.63	0.20	0.12	11.28	1.02	3.65	0.67
17a(h)-21b(h)-29-norhopane	3.87	1.07	0.50	0.39	35.33	4.00	9.82	0.46
18a(H)-29-norneohopane	0.85	0.20	0.12	0.06	5.63	1.86	1.81	0.47
17a(H)-21b(H)-hopane	3.76	1.06	0.45	0.26	30.21	6.15	8.15	1.18
17b(H),21a(H)-moretane	0.30	0.06	0.04	0.02	1.88	0.53	0.48	0.07
22S, 17a(H),21b(H)-homohopane	1.39	0.50	0.20	0.17	11.91	3.61	3.37	0.62
22R, 17a(H),21b(H)-homohopane	1.13	0.33	0.16	0.18	11.38	3.89	2.81	0.54
22S, 17a(H),21b(H)-bishomohopane	0.61	0.33	0.12	0.10	8.51	3.46	2.32	0.79
22R, 17a(H),21b(H)-bishomohopane	0.53	0.14	0.10	0.07	5.22	1.58	1.79	0.77
22S, 17a(H),21b(H)-trishomohopane	0.47	0.11	0.09	0.07	5.75	1.64	0.99	0.09
22R, 17a(H),21b(H)-trishomohopane	0.27	0.08	0.05	0.02	3.98	1.52	0.73	0.19
20R+S, abb-cholestane	0.24	0.10	0.01	0.01	1.02	0.47	0.44	0.23
20R, aaa-cholestane	1.33	0.36	0.21	0.14	10.89	1.99	3.58	0.78
20R+S, abb-ergostane	0.45	0.27	0.09	0.03	3.07	1.09	1.43	0.75
20R+S, abb-sitostane	2.08	0.56	0.34	0.20	20.33	4.67	5.83	0.96
UCM	14893.03	5365.50	2531.00	2036.95	165124.63	38365.16	53779.13	5552.17

[a] Note: Light MW PAHs (with MW $\leq$ 216) may have adsorption artifact up to 50% in ultrafine size modes.

of CO_2 and CO (μg of Carbon/m^3) above the tunnel entrance, and w_c is the weight fraction of carbon in the fuel (*2*, *30*).

To derive HDV and LDV specific emission factors, $\Delta[P]$, $\Delta[CO_2]$, and Δ[CO] must be apportioned between HDV and LDV contributions. Ignoring the very low numbers of diesel vehicles in bore 2, $\Delta[P]_{LDV}$, $\Delta[CO_2]_{LDV}$, and $\Delta[CO]_{LDV}$ are assumed to be equal to the measured concentrations in bore 2. $\Delta[CO_2]_{HDV}$ is calculated based on fuel consumption rates, fuel densities, vehicle counts, and w_c as described in Kirchstetter et al. (*30*). The calculation to determine the pollutants emitted by HDV essentially reduces to the following equation:

$$\Delta[P]_{HDV} = \Delta[P]_{bore1} - X\,\Delta[P]_{bore2}$$

which subtracts the LDV emissions as determined in bore 2 from those in bore 1. In the Kirchstetter et al. (*30*) method, which was applied here, the factor X is based on measured CO levels and vehicles count, resulting in a value of 0.86 in our study.

Results and Discussion

Tunnel Concentrations. The measured concentrations of each organic species were found to be higher at the east end than the west end, confirming significant contributions from the vehicles in the tunnel (See Table S2, Supporting Information). Most of the organic species were measured to be an order of magnitude higher in ultrafine mode than the accumulation mode; an expected result given the smaller sized primary particles emitted by vehicles. However, tunnel concentrations of particulate mass were about equivalent or at least of the same order of magnitude in both the size fractions (*2*). Bore 1 concentrations of the organic species are significantly greater than the respective Bore 2 concentrations, showing the relatively higher contribution of HDVs in Bore 1 to emissions of these species.

Table 1 shows the Pearson correlation coefficients between the measured mass concentrations of certain organic species and classes in both the size modes. The measurements made at the tunnel entrance can also be considered samples heavily influenced by traffic emissions. Therefore, all concentration data from individual days, from both bores and both ends of the tunnel, are included in the correlation calculations. The interspecies correlation among all the measured hopanes and steranes (Hop-Ster) is very high with a minimum r of 0.86 and an average r of 0.96 in the ultrafine mode (minimum $r = 0.72$, average $r = 0.91$ in the accumulation mode). Hence, the sum of the hopanes and steranes is used for comparison rather than individual species. Lower molecular weight PAHs and their methyl derivatives have been found to predominantly come from HDVs, while higher molecular weight PAHs such as benzo(ghi)perylene (BgP) and coronene (Cor) have been attributed to LDVs (*31*, *32*,

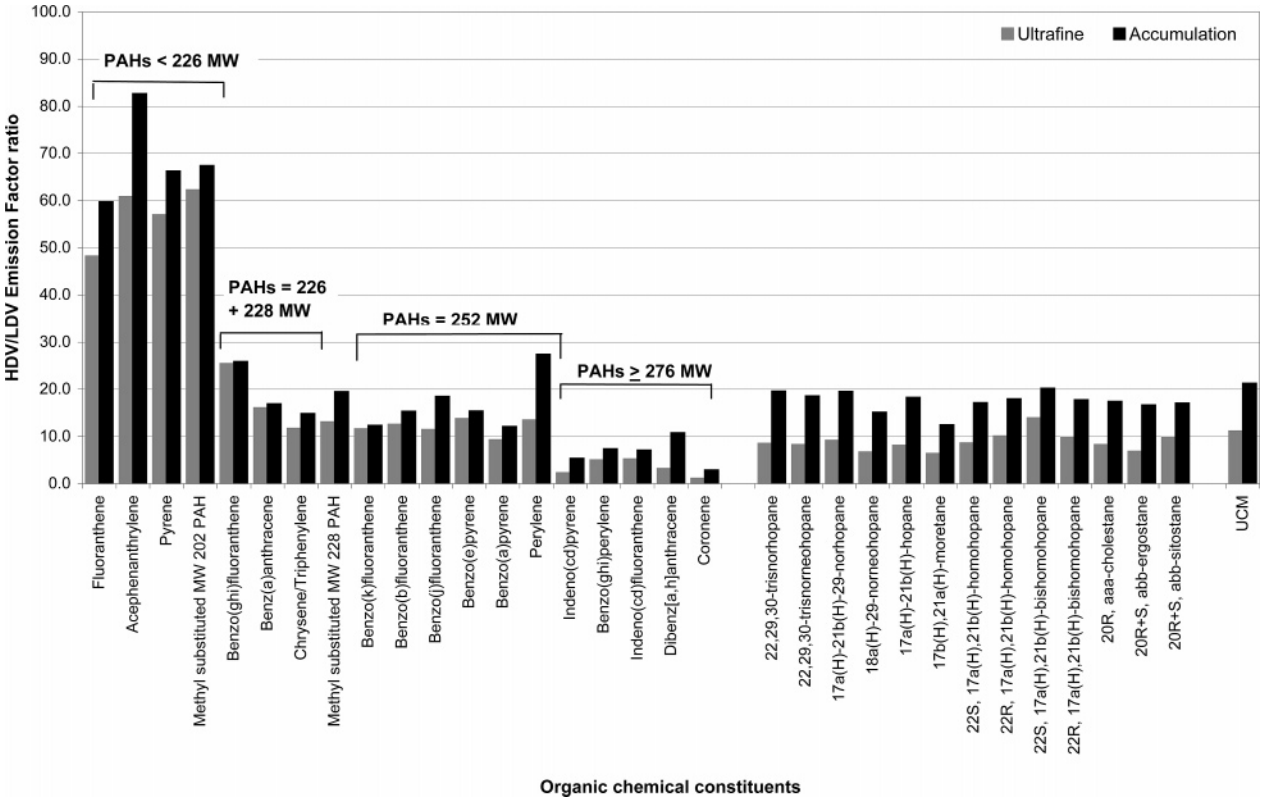

FIGURE 3. HDV/LDV emission factor ratios for the measured organics species. Note: EF ratio for PAHs <226 may be overestimated due to positive adsorption artifact in ultrafine size modes.

59). On the basis of these previous findings, we have grouped the PAHs into three groups based on their molecular weights: PAHs MW = 226 + 228 (sum of the PAHs with molecular weights 226 and 228), PAHs MW = 252, and PAHs MW ≥ 276. Coronene and benzo(ghi)perylene are included individually since they have been proposed as indicators of LDV emissions. It should be noted that this grouping of individual species does not change the correlations significantly since the species within each group are highly correlated with one another.

In general, elemental carbon (EC) is found to have good correlation with all the other parameters presented in the Table 1 in both the ultrafine and accumulation modes. The correlation is greater in the ultrafine mode than the accumulation mode, as EC and the other species are predominantly found in the ultrafine mode where nonvehicular background contributions are negligible. The lowest correlations with EC are found for the heavier PAHs. Diesel HDVs are known to emit much higher amounts of EC, while gasoline powered LDVs have been shown to emit relatively high amounts of heavier PAHs. The lower correlations can thus be attributed to two different sources of these species. Higher correlations between EC and the lighter PAHs are consistent with the previous work showing that HDVs emit relatively more light PAHs than LDVs. Figure 1 further demonstrates the correlation between EC and lighter PAHs (MW = 226 + 228). It should be noted that the levels observed at the east end of Bore 2 are higher than those that can be attributed to the few (0.4%) diesel vehicles that passed through Bore 2. The EC and light PAH concentrations in Bore 2 are approximately 25% that of the Bore 1, but the HDV traffic in Bore 2 was 10% of that observed in Bore 1. Although there was more traffic in Bore 2, the high EC and lighter PAH levels in bore 2 cannot be attributed completely to HDVs. This may indicate that the fleet of gasoline vehicles also emits EC and lighter PAHs, albeit in lower amounts per vehicle, but with a ratio similar to that observed for HDVs. It is possible that that the formation mechanisms of these two species are similar in both HDV and LDV engines. The west end concentrations depicted in the figure inset appear more enriched in EC than the east end, but they lie within the error of the best-fit linear regression parameters.

Both the unresolved complex mixture (UCM) and the hopanes and steranes derive from the same petroleum source (lubricating oil), and thus a very high correlation is observed between the two in both size ranges (*24*, *25*). Figure 2a and b display the scatter-plots demonstrating this correlation in both size modes. Again, all daily data points from both bores and tunnel ends are included. The high correlation between UCM and the hopanes/steranes implies a similar origin (lubricating oil components), and suggests that the particulate emission processes responsible for these two potential tracers are the same in both HDV and LDV.

Size-Resolved Emission Factors. Table 2 presents the size-resolved emission factors with standard deviations attributed to LDVs and HDVs for the measured organic markers. All of the emissions factors of the organic markers predominantly exist in ultrafine mode in both vehicle classes. Higher molecular weight PAHs such as BgP (9.63 ± 2.76 mg/kg fuel burned) and Cor (5.32 ± 1.00 mg/kg fuel burned) are the most abundant species emitted from LDVs, along with medium weight benzo[*a*]pyrene (BaP) (5.08 ± 1.56 mg/kg fuel burned) in the ultrafine mode. Similarly, in the accumulation mode, the highest emission factors from LDVs are found for BgP (0.68 + −0.22 mg/kg fuel burned). Conversely, HDVs emit more of the lighter molecular weight PAHs (i.e., fluoranthene, pyrene, and methyl-substituted flu/pyr) in both the ultrafine and accumulation size modes relative to the heavier PAHs. However high BgP emissions were also calculated in both modes from HDVs. Even though HDV PAH emission factors are generally larger than those for LDV, LDV emissions are enriched in heavier PAH relative to total emitted mass or total PAH emissions, while HDV emit more light PAH relative to total emissions. Comparison

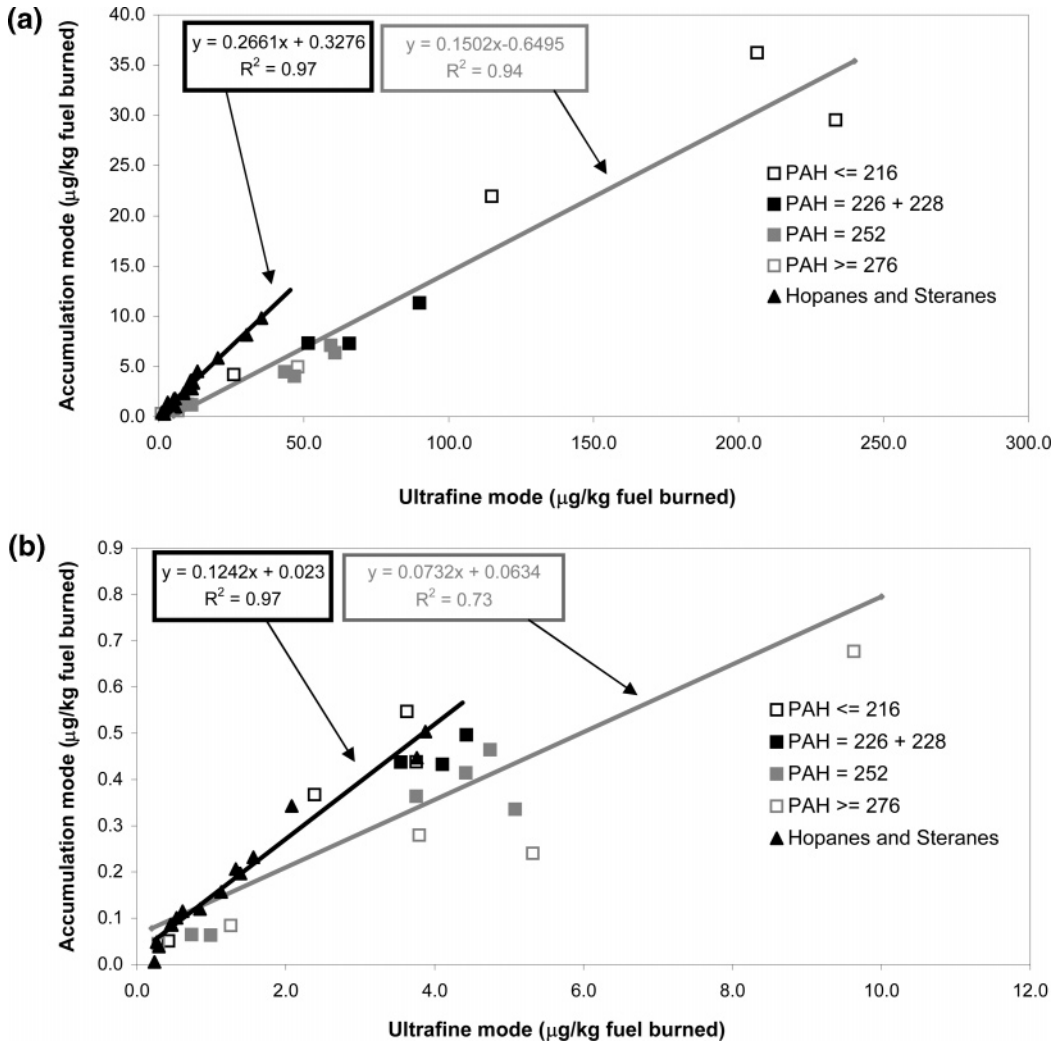

FIGURE 4. Correlation between ultrafine and accumulation mode PAHs, hopanes, and steranes for (a) HDVs and (b) LDVs. Note: PAHs ≤ 216 MW may have adsorption artifact up to 50% in ultrafine size modes.

of these calculated emission factors to earlier studies measuring $PM_{2.5}$ emissions, is presented later in the text.

Hopanes and steranes are emitted from both types of vehicles, but the relative emission factors are higher for HDVs. The predominant species in both size modes and from both types of vehicles are 17a(H)-21b(H)-29-norhopane and 17a(H)-21b(H)-hopane. In general, the LDVs emission factors are an order of magnitude less than that of the HDVs for all the hopanes and steranes. UCM shows the same trends with size and vehicle type as hopanes and steranes, which is expected due to their similar origins in lubricating oil.

Figure 3 shows the ratio of emission factors between HDV and LDV of the measured organic markers for both the size ranges. The HDV/LDV emission factor ratio of lighter PAHs (MW ≤ 216) is very high (60 to 90) as compared to the higher molecular weight ones (MW ≥ 276) (<10) for both the size ranges. The results demonstrate that lower molecular weight PAHs are emitted in relatively higher amounts by HDVs than the higher molecular weight PAHs. While HDVs emit much more PM mass and PAHs overall, the distribution of the PAHs with molecular weight is very different between HDV and LDV. Such differences may prove useful in source apportionment calculations attempting to distinguish the contributions of diesel and gasoline vehicles to ambient samples. Hopanes, steranes, and UCM are emitted from both LDVs and HDVs with similar species distributions. The relative emission factors between HDVs and LDVs lie in relatively narrow ranges, with ratios of 6−14 for the ultrafine mode and 12−21 for the accumulation mode. These ratios are more similar to the medium MW PAH than for the lighter or heavier PAHs. It can also be seen that this ratio is higher in all cases for the accumulation mode relative to the ultrafine mode, indicating HDV emissions are shifted to larger particle sizes than LDVs.

To further demonstrate the particle size partitioning for these organic species, Figure 4a and b presents the correlation between the ultrafine and accumulation mode emission factors of PAHs and hopanes and steranes from LDVs and HDVs. The high correlations for HDV show that high emissions of a particular species in one mode are accompanied by high emissions in the other mode, indicating similar size distributions for these species. The slopes less than unity show that most of the species are in the ultrafine mode, but the higher slope for the hopanes and steranes relative to the PAHs indicates that the size distribution of PAHs is shifted to smaller particle sizes than the size distribution of hopanes and steranes. Note also that the ratio of accumulation to ultrafine mode HDV emission factors for UCM is 0.33, closer to the hopanes/steranes slope of 0.27 than the PAH slope of 0.15. For the LDVs, there is more scatter in the PAH emission factor size distributions, but the hopanes/steranes are again shifted to the larger particles relative to most PAHs.

In the case of HDVs, all the PAHs, regardless of molecular weight, are found to partition between ultrafine and accumulation modes in similar ways. But it is apparent in Figure

TABLE 3. Comparison of Particle Phase PM2.5 Emission Factors (in μg/kg Fuel Burned) Attibutable to LDVs[a]

organic compounds	this study	Zielinska et al., 2004[b] cat.	Zielinska et al., 2004[b] noncat.[c]	Schauer et al., 2002[d] cat.	Schauer et al., 2002[d] noncat.	Rogge et al., 1993[e] cat.	Rogge et al., 1993[e] noncat.	Marr et al., 1999[f]	Miguel et al., 1998[g]
PAHs									
fluoranthene	2.75	416.44	2759.67	0.78	1,711.71	22.52	543.92	8	10.3
acephenanthrylene	0.48			0.14	650.90				
pyrene	4.17	195.27	1568.46	0.87	2,443.69	28.15	349.10	9.00	13.80
methyl substituted MW 202 PAH	4.19	356.24	5260.04		2,623.87	47.30	1203.83		
benzo(ghi)fluoranthene	3.98			0.71	527.03	14.64	278.15		
benz[*a*]anthracene	4.54	37.02	573.35	1.09	584.46	21.40	831.08	4.80	8.80
chrysene/triphenylene	4.92	54.38	828.15	2.32	586.71	42.79	628.38	7.00	8.60
methyl substituted MW 228 PAH	3.34			2.73	1,159.91	38.29	1615.99		
benzo[*k*]fluoranthene	4.12			0.93	368.24	22.52	458.33	2.50	3.00
benzo[*b*]fluoranthene	5.21	23.17	476.63		420.05	32.66	426.80	7.60	8.10
benzo[*j*]fluoranthene	1.06			0.10	17.12	6.08	67.57		
benzo[*e*]pyrene	4.84	13.93	293.81	1.69	430.18	22.52	515.77		
benzo[*a*]pyrene	5.42	12.74	328.91	0.24	461.71	21.40	489.86	6.40	8.30
perylene	0.80			0.35		6.76	157.66		
indeno(cd)pyrene	4.07	10.36	243.95	4.91	1,036.04	5.29	72.07		
benzo(ghi)perylene	10.31	16.24	428.05			52.93	1637.39	18.00	20.70
indeno(cd)fluoranthene	1.35					19.14	367.12	9.00	7.50
dibenz[a,h]anthracene	0.34	2.10	47.00			3.72	93.47	16.20	1.30
coronene	5.56	7.14	84.44		1,137.39	12.39	1177.93		
Hopanes and Steranes									
22,29,30-trisnorhopane	1.80	0.07	9.03		777.03				
22,29,30-trisnorneohopane	1.57	6.02	286.82	0.43	1,407.66	76.58	33.78		
17a(H)-21b(H)-29-norhopane	4.38	3.57	235.41	0.21	3,175.68	120.50	66.44		
17a(H)-21b(H)-hopane	4.21	0.14	22.40	0.37	3,614.86	204.95	101.35		
17b(H),21a(H)-moretane	0.34	0.21	39.05						
22S, 17a(H),21b(H)-homohopane	1.59	1.19	116.04		2,916.67	93.47	34.91		
22R, 17a(H),21b(H)-homohopane	1.29	0.84	84.83			61.94	21.40		
22S, 17a(H),21b(H)-bishomohopane	0.73	0.49	65.44		2,207.21	52.93	16.89		
22R, 17a(H),21b(H)-bishomohopane	0.64	0.42	44.48			39.41	12.39		
22S, 17a(H),21b(H)-trishomohopane	0.56	0.28	49.87						
22R, 17a(H),21b(H)-trishomohopane	0.31	0.14	31.81						
20R+S, abb-cholestane	0.24	1.61	94.84	1,914.41	94.59	40.54			
20R, aaa-cholestane	1.53			1,340.09	104.73	45.05			
20R+S, abb-ergostane	0.54			1,565.32	88.96	46.17			
20R+S, abb-sitostane	2.42	1.19	92.70	1,531.53	128.38	60.81			

[a] Note: Light MW PAHs (with MW <= 216) may have adsorption artifact up to 50% in ultrafine size modes. [b] Run on California unified driving cycle (UDC); 5 catalyst-equipped vehicles (1993−1996 model year); 2 noncatalyst (1976 model year black emitter and 1990 model year white emitter). [c] Average of black emitter and white emitter gasoline vehicles. [d] Run on cold-start FTP urban driving cycle; 9 catalyst-equipped with average model year 1990 (1981−1994) and 2 1970 model year noncatalyst vehicles. [e] Run on cold-start FTP urban driving cycle; 5 catalyst-equipped vehicles (model year 1977−1983) and 6 noncatalyst (model year 1965−1976). [f] 1997 data from Caldecott tunnel with %HD diesel = 4.3. [g] 1996 data from Caldecott tunnel with %HDVs = 4.7.

4b that for LDVs the lighter PAHs tend to be more associated with larger particles than the heavier PAH, suggesting that the volatility of a particular species affects its size distribution. This observation is in agreement with earlier reported studies that the more volatile PAHs tend to partition into higher particle size fractions (*31*, *32*). As suggested in Figure 4, all HDV emission factors result in higher slopes than LDVs, indicating that HDV emissions are shifted to larger sizes relative to LDV emissions. This is somewhat expected given the agglomerate nature of soot particles emitted from diesel engines which can have larger aerodynamic diameters than the nucleation mode gasoline emissions (*21*, *60*).

Comparison with Other Studies. Tables 3 and 4 compare the LDV and HDV $PM_{2.5}$ emission factors from this study (accumulation plus ultrafine modes) to other earlier studies, including tunnel and chassis dynamometer studies. It is immediately evident that there are large differences in reported emission factors from various studies. Testing an individual vehicle, or even averaging over several vehicles, can lead to very different results than a tunnel study that includes an average over thousands of vehicles. Miguel et al. (*32*) and Marr et al. (*31*) have reported PAHs emissions from the Caldecott tunnel measured in 1996 and 1997, respectively. Miguel et al. (*32*) have reported $PM_{1.3}$ emission factors for particulate PAHs and it can be seen that for the LDVs there is a modest decrease in the PAHs emission factors between 1996 and the current 2004 study. This may be due to better control technologies, but is more likely due to the removal of older high-emitting vehicles from the on-road fleet during the seven years between the measurements. Reformulated gasoline (RFG) was introduced in the San Francisco Bay Area in 1996, which resulted in significant reductions in overall pollutant emissions. Kirchstetter et al. (*55*) have attributed this reduction in pollutant emissions from vehicles to both fleet turnover and the introduction of RFG. The 1997 study by Marr et al. (*31*) in the same tunnel also showed a slight reduction in PAHs emissions as compared to the previous 1996 study by Miguel et al. (*32*). For HDVs, the lighter PAHs emissions were lower in this study as compared to both of the 1996 and 1997 studies. However, in both of these studies they did not attribute the higher molecular weight PAHs to HDVs, while we attribute significant emissions of the higher PAHs to HDVs. Zielinska et al. (*26*), also measured heavier PAH in the emissions from diesel vehicles (coronene and BgP), and Rogge et al. (*23*), also found BgP in diesel emissions.

The other tunnel studies are from Chellam et al. (*28*) in a Houston tunnel and Fraser et al. (*29*) in a Los Angeles tunnel. Both of these studies reported mixed fleet (LDVs + HDVs) emission factors for the organic markers. The PAH emission factors from the Houston tunnel are generally between our LDVs and HDVs emission factors, with the exception of dibenz(a,h)anthracene, which had a higher emission factor

TABLE 4. Comparison of Particle Phase PM 2.5 Emission Factors (in μg/kg Fuel Burned) Attributable to HDVs and Mixed Tunnel Fleets[a]

	HDVs						Mixed tunnel fleet	
organic compounds	this study	Zielinska et al., 2004[b]	Schauer et al., 1999[c]	Rogge et al., 1993[d]	Marr et al., 1999[e]	Miguel et al., 1998[f]	Chellam et al., 2005[g,i]	Fraser et al., 1998[h,i]
PAHs								
fluoranthene	136.83	32.51	143.36	32.93	480.00	749.00	18.90	4.85
acephenanthrylene	30.09		41.03					1.48
pyrene	242.70	44.24	224.16	57.24	690.00	986.00	21.37	8.35
Methyl substituted MW 202 PAH	263.06	31.25	205.17	32.42				27.74
benzo(ghi)fluoranthene	101.30		50.15	17.48				26.53
benz[*a*]anthracene	72.99	2.76	19.66	9.12	140.00	180.00	5.62	28.14
chrysene/triphenylene	58.85	7.71	39.51	25.08	66.00	140.00	20.16	32.05
Methyl substituted MW 228 PAH	45.12		16.57	6.84				90.09
benzo[*k*]fluoranthene	47.87			6.84	2.80	59.00	8.94	21.28
benzo[*b*]fluoranthene	66.46	3.59		7.35	25.00	90.00	11.44	
benzo[*e*]pyrene	67.16	2.08		6.59			13.56	29.22
benzo[*a*]pyrene	50.80	6.79		3.29		126.00	5.32	24.64
perylene	11.24			2.53			3.11	5.25
indeno(cd)pyrene	10.01	0.91					5.32	41.21
benzo(ghi)perylene	52.86	2.15		4.05			10.96	137.62
indeno(cd)fluoranthene								14.00
dibenz[a,h]anthracene	1.28	0.14					7.38	
coronene	1.94	1.27						
Hopanes and Steranes								
22,29,30-trisnorhopane	17.80	8.66	2.51				15.99	24.24
22,29,30-trisnorneohopane	14.93	102.88	6.94	58.51			15.24	37.71
17a(H)-21b(H)-29-norhopane	45.15	5.61	28.62	100.30			45.05	73.53
18a(H)-29-norneohopane	7.44						11.05	21.01
17a(H)-21b(H)-hopane	38.36	7.23	28.88	238.60			53.98	110.42
17b(H),21a(H)-moretane	2.24	4.20						
22S, 17a(H),21b(H)-homohopane	15.29	48.65		96.25			18.34	46.73
22R, 17a(H),21b(H)-homohopane	14.18	33.17		97.01			14.96	31.38
22S, 17a(H),21b(H)-bishomohopane	10.84	49.99		57.50			10.89	29.36
22R, 17a(H),21b(H)-bishomohopane	7.01	31.52		40.53			8.11	18.85
22S, 17a(H),21b(H)-trishomohopane	6.74	14.66						
22R, 17a(H),21b(H)-trishomohopane	3.72	8.74						
20R+S, abb-cholestane	1.46	28.53	1.98	100.30				15.35
20R, aaa-cholestane	14.47		3.01	108.92				23.70
20R+S, abb-ergostane	4.50		7.98	109.93				30.03
20R+S, abb-sitostane	26.16	31.71	6.61	160.59				28.82
UCM	218903.76		104863.22					

[a] Note: Light MW PAHs (with MW <= 216) may have adsorption artifact up to 50% in ultrafine size modes. [b] Run on California unified driving cycle (UDC); 4 diesel vehicles (model year 1991−2000). [c] Run on hot-start FTP urban driving cycle; 2 medium duty diesel trucks. [d] 2 Diesel trucks (1987 model year). [e] 1997 data from Caldecott tunnel with %HDVs = 4.3. [f] 1996 data from Caldecott tunnel with %HDVs = 4.7. [g] 2000 Houston tunnel study; %HDVs = 3.4 [h] 1993 Los Angeles tunnel study with average 1986 model year vehicles; % HDVs = 2.7 and % noncatalyst vehicles = 3.6. [i] Tunnel study with mixed fleet, hence mixed fleet (LDV + HDV) emision factors are reported.

from the Houston tunnel than that of what was attributed to HDVs here. However, the hopanes/steranes emissions in the Houston tunnel are very similar to our results for HDV from the Caldecott tunnel. Differences may also be due to different vehicle types, fuel blends, tunnel characteristics, or average speeds. Also, the Houston tunnel study occurred at different times over different days whereas the current study sampled over the same time period every day. The Van Nuys tunnel study in 1993 by Fraser et al. (*29*) shows higher levels of higher molecular weight PAHs emissions as well as higher hopanes/steranes emissions compared to our study. The lighter PAHs, however, are much less compared to our HDVs contributions. Again, there are many possible reasons for these discrepancies, including higher numbers of older or noncatalytic cars, different vehicle driving conditions, and fuel composition.

Table 3 shows three chassis dynamometer studies done in 1993, 2002, and 2004 for LDVs. Compared to the Schauer et al. (*25*) study, our LDV emission factor values fall between the catalyst and noncatalyst emissions for all the measured species, as one would expect in a tunnel with mostly catalyst but some noncatalyst (or malfunctioning catalyst) vehicles as well. The higher catalyst emissions from Rogge et al. (*23*) may be due to the pre-reformulation gasoline and possibly less advanced control technologies at the time of that study. Zielinska et al. (*26*) fine PAHs emission factors for the catalyst-equipped vehicles are higher than the LDVs emission factor reported in this study. Since all of the dynamometer testing occurs over specified driving cycles, often including cold-start and multiple accelerations, it is not surprising that the emissions of certain species will be higher. For the HDVs, the dynamometer studies by Zielinska et al. (*26*), and Rogge et al. (*23*) resulted in generally lower PAH emissions, whereas a few of the hopanes and steranes are significantly higher in theses previous studies. A similar study by Schauer et al. (*24*), however, is very close to our results for the lighter PAHs and the hopanes and steranes, but no higher molecular weight PAHs were reported.

Uncertainty Analysis. The main source of error in HDV apportionment arises from the value of *X*, which relates to the uncertainty in measurement of CO and CO_2, and vehicle count. In our study the uncertainty in vehicle counting is not more than 10%, which does not make any significant difference in *X* as the fraction of diesel vehicles is very low in the tunnel. For CO and CO_2 measurements the uncertainty in our case is <5%, which adds to <8% uncertainty in *X*. Light-duty gasoline vehicles and heavy-duty diesel trucks have been shown to emit comparable amounts of CO per

unit mass traveled in previous tunnel studies (*30*, *61*). On-road measurements on California freeways by Westerdahl et al. (*62*) also corroborate these findings, showing comparable CO concentrations in Los Angeles freeways dominated by HDV or LDV vehicles. Hence, the assumption of similar CO emissions from gasoline and diesel vehicles does not introduce significant error in apportioning the HDV emissions.

The main source of error in LDV emissions estimates derives from the few diesel vehicles (less than 10% of that in bore 1) that passed through bore 2. The presence of diesel vehicles in bore 2 does not significantly affect the HDV emissions estimates, which therefore can be used to assess the impact of bore 2 diesel vehicles on calculated LDV emission factors. For the worst case of the light PAH emission factors, specifically fluoranthene, pyrene, and PAHs with MW 216, the diesel vehicles in bore 2 can add as much as 19−24% uncertainty to the LDV results in the ultrafine mode. For all the other organic species, the error introduced is less than 10%. Due to the extremely low counts of HDV in bore 2, and the uncertainty in the 2-axle/6-tire split assumptions, it is not feasible to correct LDV emissions factors based on our HDV results. Thus, the cumulative uncertainty including the analytical measurement errors in LDV emissions factors may be as much as 50% for light MW PAHs in ultrafine mode. As reported in the previous Caldecott tunnel studies (*2*, *30*) the HDV apportionment is also affected by the use of measured Fort McHenry tunnel fuel economies for the Caldecott tunnel vehicles as well as the classification of 2-axle/6-tire trucks as gasoline or diesel powered.

Acknowledgments

We thank Satya B. Sardar at USC for assistance in the sampling campaign, Meg Krudysz at UCLA for help with the sample extractions, and James J. Schauer at the University of Wisconsin for providing the organic standard mixtures, and the Caltrans Caldecott Tunnel crew. This research was supported by the Southern California Particle Center and Supersite (SCPCS), funded by the USEPA under the STAR program (STAR award R82735201). The research described herein has not been subjected to the agency's required peer and policy review and therefore does not necessarily reflect the views of the agency, and no official endorsement should be inferred. Mention of trade names or commercial products does not constitute an endorsement or recommendation for use.

Supporting Information Available

Tables of tunnel traffic volumes and mean mass concentrations of measured species in Bores 1 and 2. This material is available free of charge via the Internet at http://pubs.acs.org.

Literature Cited

(1) Abu-Allaban, M.; Coulomb, W.; Gertler, A. W.; Gillies, Pierson, J. W. R.; Rogers, C. F.; Sagebiel, J. C.; Tarnay, L. Exhaust particle size distribution measurements at the Tuscarora mountain tunnel. *Aerosol Sci. Technol.* **2002**, *36*, 771−789.

(2) Geller, M. D.; Sardar, S. B.; Phuleria H. C.; Fine P. M.; Sioutas, C. Measurements of particle number and mass concentrations and size distributions in a tunnel environment. *Environ. Sci. Technol.* **2005**, *39*, 8653−8663.

(3) Lighty, J. B.; Veranth, J. M.; Sarofim, A. F. Combustion aerosols: Factors governing their size and composition and implications to human health. *J. Air Waste Manage. Assoc.* **2000**, *50*, 1565−1618.

(4) Mauderly, J. L. Toxicological approaches to complex mixtures. *Environ. Health Perspect.* **1993**, *101*, 155−165.

(5) Mauderly, J. L. Toxicological and epidemiological evidence for health risks from inhaled engine emissions. *Environ. Health Perspect.* **1994**, *102*, 165−171.

(6) Weingartner, E.; Keller, C.; Stahel, W. A.; Burtscher, H.; Baltensperger, U. Aerosol emission in a road tunnel. *Atmos. Environ.* **1997**, *31* (3), 451−462.

(7) Li, N.; Sioutas, C.; Cho, A.; Schmitz, D.; Misra, C.; Sempf, J.; Wang, M. Y.; Oberley, T.; Froines, J.; Nel, A. Ultrafine particulate pollutants induce oxidative stress and mitochondrial damage. *Environ. Health Perspect.* **2003**, *111* (4), 455−460.

(8) Xia, T.; Korge, P.; Weiss, J. N.; Li, N.; Venkatesen, I. M.; Sioutas, C.; Nel A. Quinones and aromatic chemical compounds in particulate matter induce mitochondrial dysfunction: Implications for ultrafine particle toxicity. *Environ. Health Perspect.* **2004**, *112* (14), 1347−1358.

(9) Johnston, C. J.; Finkelstein, J. N.; Mercer, P.; Corson, N.; Gelein, R.; Oberdorster, G. Pulmonary Effects Induced by Ultrafine PTFE Particles. *Toxicol. Appl. Pharmacol.* **2000**, *168*, 208−215.

(10) Kleinman, M. T.; Sioutas, C.; Chang, M. C.; Boere, A. J. F.; Cassee, F. R. Ambient fine and coarse particle suppression of alveolar macrophage functions. *Toxicol. Lett.* **2003**, *137*, 151−158.

(11) Kleinman, M. T.; Hamade, A.; Meacher, D.; Oldham, M.; Sioutas, C.; Chakrabarti, L.; Stram, D.; Froines, J. R.; Cho, A. K. Inhalation of concentrated ambient particulate matter near a heavily trafficked road stimulates antigen-induced airway responses in mice. *J. Air Waste Manage. Assoc.* **2005**, *55* (9), 1277−1288.

(12) Oberdorster, G. Pulmonary effects of inhaled ultrafine particles. *Int. Arch. Occupat. Environ. Health.* **2001**, *74*, 1−8.

(13) Oberdorster, G.; Sharp, Z.; Atudorei, V.; Elder, A.; Gelein, R.; Lunts, A.; Kreyling, W.; Cox, C. Extrapulmonary translocation of ultrafine carbon particles following whole-body inhalation exposure of rats. *J. Toxicol. Environ. Health, Part A* **2002**, *65*, 1531−1543.

(14) Chakrabarti, B.; Singh, M.; Sioutas, C. Development of a near-continuous monitor for measurement of the sub-150 nm PM mass concentration. *Aerosol Sci. Technol.* **2004**, *38*, 239−252.

(15) Fine, P. M.; Chakrabarti, B.; Krudysz, M.; Schauer, J. J.; Sioutas, C. Diurnal variations of individual organic compound constituents of ultrafine and accumulation mode particulate matter in the Los Angeles Basin. *Environ. Sci. Technol.* **2004**, *38*, 1296−1304.

(16) Sardar, S. B.; Fine, P. M.; Yoon, H.; Sioutas, C. Associations between particle number and gaseous co-pollutant concentrations in the Los Angeles Basin. *J. Air Waste Manage. Assoc.* **2004**, *54*, 992−1005.

(17) Janhall, S.; Jonsson, A. M.; Molnar, P.; Svensson, E. A.; Hallquist, M. Size resolved traffic emission factors of submicrometer particles. *Atmos. Environ.* **2004**, *26*, 4331−4340.

(18) Sioutas, C.; Delfino, R. J.; Singh M. Exposure assessment for atmospheric ultrafine particles (UFPs) and implications in epidemiologic research. *Environ. Health Perspec.* **2005**, *113*, 947−955.

(19) Kuhn, T.; Biswas, S.; Fine, P. M.; Geller, M.; Sioutas, C. Physical and chemical characteristics and volatility of PM in the proximity of a light-duty vehicle freeway. *Aerosol Sci. Technol.* **2005**, *39* (4), 347−357.

(20) Canagaratna, A.; Jayne, J.; Ghertner, D.; Herndon, S.; Shi, Q.; Jimenez, J.; Silva, P.; Williams, P.; Lanni, T.; Drewnick, F.; Demerjian, K.; Kolb, C.; Worsnop D. Chase studies of particulate emissions from in-use New York city vehicle. *Aerosol Sci. Technol.* **2004**, *38*, 555−573.

(21) Kittelson, D. B., Engines and nanoparticles: A review. *J. Aerosol Sci.* **1998**, *29*, 575−588.

(22) Gross, D. S.; Barron, A. R.; Sukovich, E. M.; Warren, B. S.; Jarvis, J. C.; Suess, D. T.; Prather, K. A. Stability of single particle tracers for differentiating between heavy- and light-duty vehicle emissions. *Atmos. Environ.* **2005**, *39* (16), 2889−2901.

(23) Rogge W. F.; Hildemann, L. M.; Mazurek, M. A.; Cass, G. R.; Simoneit, B. R. T. Sources of fine organic aerosol. 2. Noncatalyst and catalyst-equipped automobiles and heavy-duty diesel trucks. *Environ. Sci. Technol.* **1993**, *27*, 636−651.

(24) Schauer, J. J.; Kleeman, M. J.; Cass, G. R.; Simoneit, B. R. T. Measurement of emissions from air pollution sources. 2. C_1 through C_{30} organic compounds from medium duty diesel trucks. *Environ. Sci. Technol.* **1999**, *33*, 1578−1587.

(25) Schauer, J. J.; Kleeman, M. J.; Cass, G. R.; Simoneit, B. R. T. Measurement of emissions from air pollution sources. 5. C_1−C_{32} organic compounds from gasoline-powered motor vehicles. *Environ. Sci. Technol.* **2002**, *36*, 1169−1180.

(26) Zielinska, B.; Sagebiel, J.; McDonald, J. D.; Whitney, K.; Lawson, D. R. Emission rates and comparative chemical composition from selected in-use diesel and gasoline-fueled vehicles. *J. Air Waste Manage. Assoc.* **2004**, *54*, 1138−1150.

(27) Allen, J. O.; Mayo, P. R.; Hughes, L. S.; Salmon, L. G.; Cass, G. R. Emissions of size-segregated aerosols from on-road vehicles in the Caldecott tunnel. *Environ. Sci. Technol.* **2001**, *35*, 4189−4197.
(28) Chellam, S.; Kulkarni, P.; Fraser, M. P. Emissions of organic compounds and trace metals in fine particulate matter from motor vehicles: A tunnel study in Houston, Texas. *J. Air Waste Mange. Assoc.* **2005**, *55*, 60−72.
(29) Fraser, M. P.; Cass, G. R.; Simoneit, B. R. T. Gas-phase and particle-phase organic compounds emitted from motor vehicle traffic in a Los Angeles roadway tunnel. *Environ. Sci. Technol.* **1998**, *32*, 2051−2060.
(30) Kirchstetter, T. W.; Harley, R. A.; Kreisberg, N. M.; Stolzenburg, M. R.; Hering, S. V. On-road measurement of fine particle and nitrogen oxide emissions from light- and heavy-duty motor vehicles. *Atmos. Environ.* **1999**, *33*, 2955−2968.
(31) Marr, L. C.; Kirchstetter, T. W.; Harley, R. A.; Miguel, A. H.; Hering, S. V.; Hammond, S. K. Characterization of polycyclic aromatic hydrocarbons in motor vehicle fuels and exhaust emissions. *Environ. Sci. Technol.* **1999**, *33*, 3091−3099.
(32) Miguel, A. H.; Kirchstetter, T. W.; Harley, R. A.; Hering, S. V. On-road emissions of particulate polycyclic aromatic hydrocarbons and black carbon from gasoline and diesel vehicles. *Environ. Sci. Technol.* **1998**, *32*, 450−455.
(33) Schauer, J. J.; Shafer, M.; Christensen, C.; Kittelson, D. B.; Johnson, J.; Watts, W. Impact of Cold-Cold Start Temperature on the Chemical Composition of PM Emissions from SI Vehicles. Presented at 13th CRC On-Road Vehicle Emissions Workshop, San Diego, CA, April 7−9, 2003.
(34) Mathis, U.; Ristimäki, J.; Mohr, M.; Keskinen, J.; Ntziachristos, L.; Samaras, Z.; Mikkanen, P. Sampling conditions for the measurement of nucleation mode particles in the exhaust of a diesel vehicle. *Aerosol Sci. Technol.* **2004**, *38* (12), 1149−1160.
(35) Kean, A. J.; Harley, R. A.; Kendall, G. R. Effects of vehicle speed and engine load on motor vehicle emissions. *Environ. Sci. Technol.* **2003**, *37*, 3739−3746.
(36) Dockery, D. W.; Pope, C. A.; Xu, X. P.; Spengler, J. D.; Ware, J. H.; Fay, M. E.; Ferris, B. G.; Speizer, F. E. An association between air-pollution and mortality in 6 United States cities. *New Engl. J. Med.* **1993**, *329*, 1753−1759.
(37) Mazzoleni, C.; Kuhns, H. D.; Moosmuller, H.; Keislar, R. E.; Barber, P. W.; Robinson, N. F.; Watson, J. G. On-road vehicle particulate matter and gaseous emission distributions in Las Vegas, Nevada, compared with other areas. *J. Air Waste Mange. Assoc.* **2004**, *54* (6), 711−726.
(38) Fraser, M. P.; Cass, G. R.; Simoneit, B. R. T. Air quality model evaluation data for organics. 6. C_3−C_{24} organic acids. *Environ. Sci. Technol.* **2003**, *37*, 446−453.
(39) Schauer, J. J.; Rogge, W. F.; Hildemann, L. M.; Mazurek, M. A.; Cass, G. R.; Simoneit, B. R. T. Source apportionment of airborne particulate matter using organic compounds as tracers. *Atmos. Environ.* **1996**, *30*, 3837−3855.
(40) Schauer, J. J.; Cass, G. R. Source apportionment of wintertime gas-phase and particle-phase air pollutants using organic compounds as tracers. *Environ. Sci. Technol.* **2000**, *34*, 1821−1832.
(41) Simoneit, B. R. T. Chemical characterization of submicron organic aerosols in the tropical trade winds of the Caribbean using gas chromatography−mass spectrometry. A*tmos. Environ.* **2002**, *36*, 5259−5263.
(42) Zheng, M.; Cass, G. R.; Schauer, J. J.; Edgerton, E. S. Source apportionment of $PM_{2.5}$ in the Southeastern United States using solvent-extractable organic compounds as tracers. *Environ. Sci. Technol.* **2002**, *36*, 2361−2371.
(43) Cass, G. R. Organic molecular tracers for particulate air pollution sources. *Trends Anal. Chem.* **1998**, *17* (6), 356−366.
(44) Fine, P. M.; Cass, G. R.; Simoneit, B. R. T. Chemical characterization of fine particle emissions from fireplace combustion of woods grown in the Northeastern United States. *Environ. Sci. Technol.* **2001**, *35*, 2665−2675.
(45) Schauer, J. J. Evaluation of elemental carbon as a marker for diesel particulate matter. *J. Exposure Anal. Environ. Epidemiol.* **2003**, *13*, 443−453.
(46) Fraser, M. P.; Buzcu, B.; Yue, Z. W.; McGaughey, G. R.; Desai, N. R.; Allen, D. T.; Seila, R. L.; Lonneman, W. A.; Harley, R. A. Separation of fine particulate matter emitted from gasoline and diesel vehicles using chemical mass balancing techniques. *Environ. Sci. Technol.* **2003**, *37*, 3904−3909.
(47) McGaughey, G. R.; Desai, N. R.; Allen, D. T.; Seila, R. L.; Lonneman, W. A.; Fraser, M. P.; Harley, R. A.; Pollack, A. K.; Ivy, J. M.; Price, J. H. Analysis of motor vehicle emissions in a Houston tunnel during the Texas Air Quality Study 2000. *Atmos. Environ.* **2004**, *38* (20), 3363−3372.
(48) Hays, M. D.; Smith, N. D.; Dong, Y. Nature of unresolved complex mixture in size-distributed emissions from residential wood combustion as measured by thermal desorption-gas chromatography−mass spectrometry. *J. Geophys. Res.* **2004**, *109* (D16S04).
(49) Simoneit, B. R. T. Organic-matter of the troposphere. 3. Characterization and sources of petroleum and pyrogenic residues in aerosols over the Western United States. *Atmos. Environ.* **1984**, *18* (1), 51−67.
(50) Allen, J. O.; Dookeran, K. M.; Smith, K. A.; Sarofim, A. F.; Taghizadeh, K.; Lafleur, A. L. Measurement of polycyclic aromatic hydrocarbons associated with size-segregated atmospheric aerosols in Massachusetts. *Environ. Sci. Technol.* **1996**, *30*, 1023−1031.
(51) Allen, J. O.; Dookeran, N. M.; Taghizadeh, K.; Lafleur, A. L.; Smith, K. A.; Sarofim, A. F. Measurement of oxygenated polycyclic aromatic hydrocarbons associated with a size-segregated urban aerosol. *Environ. Sci. Technol.* **1997**, *31*, 2064−2070.
(52) Allen, J. O.; Durant, J. L.; Dookeran, N. M.; Taghizadeh, K.; Plummer, E. F.; Lafleur, A. L.; Sarofim, A. F.; Smith, K. A. Measurement of $C_{24}H_{14}$ polycyclic aromatic hydrocarbons associated with a size-segregated urban aerosol. *Environ. Sci. Technol.* **1998**, *32*, 1928−1932.
(53) Garnes, L. A.; Allen, D. T. Size distributions of organonitrates in ambient aerosol collected in Houston, Texas. *Aerosol Sci. Technol.* **2002**, *36* (10), 983−992.
(54) Misra, C.; Kim, S.; Shen, S.; Sioutas, C. A high flow rate, very low-pressure drop impactor for inertial separation of ultrafine from accumulation mode particles. *J. Aerosol Sci.* **2002**, *33*, 735−752.
(55) Kirchstetter, T. W.; Singer, B. C.; Harley, R. A.; Kendall, G. R.; Traverse, M. Impact of California reformulated gasoline on motor vehicle emissions. I. Mass emission rates. *Environ. Sci. Technol.* **1999**, *33*, 318−328.
(56) Mazurek, M. A.; Simoneit, B. R. T.; Cass, G. R.; Gray, H. A. Quantitative high-resolution gas-chromatography and high-resolution gas-chromatography mass-spectrometry analyses of carbonaceous fine aerosol-particles. *Int. J. Environ. Anal. Chem.* **1987**, *29*, 119−139.
(57) Sheesley, R. J.; Schauer, J. J.; Chowdhury, Z.; Cass, G. R.; Simoneit, B. R. T. Characterization of organic aerosols emitted from the combustion of biomass indigenous to South Asia. *J. Geophys. Res., [Atmos.]* **2003**, *108*, No. 4285.
(58) Fraser, M. P.; Yue, Z. W.; Buzcu, B. Source apportionment of fine particulate matter in Houston, TX, using organic molecular markers. *Atmos. Environ.* **2003**, *37* (15), 2117−2123.
(59) Gross, D. S.; Galli, M. E.; Silva, P. J.; Wood, S. H.; Liu, D. Y.; Prather, K. A. Single particle characterization of automobile and diesel truck emissions in the Caldecott tunnel. *Aerosol Sci. Technol.* **2000**, *32* (2), 152−163.
(60) Kleeman, M. J.; Schauer, J. J.; Cass, G. R. Size and composition distribution of fine particulate matter emitted from motor vehicles. *Environ. Sci. Technol.* **2000**, *34*, 1132−1142.
(61) Pierson, W. R.; Gertler, A. W.; Robinson, N. F.; Sagebiel, J. C.; Zielinska, B.; Bishop, G. A.; Stedman, D. H.; Zweidinger, R. B.; Ray, W. D. Real-world automotive emissions − summary of studies in the Fort McHenry and Tuscarora Mountain tunnels. *Atmos. Environ.* **1996**, *30*, 2233−2256.
(62) Westerdahl, D.; Fruin, S.; Sax, T.; Fine, P. M.; Sioutas, C. Mobile platform measurements of ultrafine particles and associated pollutant concentrations on freeways and residential streets in Los Angeles. *Atmos. Environ.* **2005**, *39*, 3597−3610.

Received for review November 1, 2005. Revised manuscript received April 11, 2006. Accepted May 2, 2006.

ES052186D